SCIENCE CHINA
Information Sciences

• LETTER •

March 2022, Vol. 65 139302:1–139302:2
https://doi.org/10.1007/s11432-020-3231-6

Design of a UCA structure with maximum capacity for mmWave LOS MIMO systems

Jiancun FAN[1*], Hongji LIU[1], Jie LUO[1], Xinmin LUO[1*] & Jinbo ZHANG[2]

[1] *The School of Information and Communications Engineering, Xi'an Jiaotong University, Xi'an* 710049*, China;*
[2] *The 54th Research Institute of CETC (CETC-54), Shijiazhuang* 050081*, China*

Received 30 November 2020/Revised 16 February 2021/Accepted 26 March 2021/Published online 10 February 2022

Citation Fan J C, Liu H J, Luo J, et al. Design of a UCA structure with maximum capacity for mmWave LOS MIMO systems. Sci China Inf Sci, 2022, 65(3): 139302, https://doi.org/10.1007/s11432-020-3231-6

Dear editor,

In millimeter wave (mmWave) systems, traditional multiple input multiple output (MIMO) may become line-of-sight (LOS) MIMO [1], and the rank of the channel matrix using the traditional antenna structure becomes very small [2]. A lower rank implies a low channel capacity [3]. The channel capacity of an LOS MIMO system can be enhanced by adjusting the array diameter of a uniform circular array (UCA), but the channel matrix cannot reach full rank when the UCA contains more than four antennas [4]. Zhu et al. [5] optimized the UCA diameter using the Newton iterative method, but their approach may require a huge antenna size to obtain small channel capacity gains. To avoid these problems, we propose a new method that designs the UCA diameter for any number of antennas. The designed size of the UCA is linearly related to the number of radio frequency (RF) chains.

System model. We developed a UCA model with N RF chains at the transmitter (Tx) and M RF chains at the receiver (Rx). Each RF chain at Tx drives one antenna, and each RF chain at Rx is connected to one antenna. The diameters of the transmitting and receiving antenna arrays are d_t and d_r, respectively. The Tx and Rx are separated by a distance L.

Channel model and design of the UCA structure. When the structure of the UCA, the carrier frequency, and the distance L are determined, the (m,n)th element of the channel matrix $\boldsymbol{H}$ is computed as

$$h_{m,n} = \mathrm{e}^{\mathrm{j}\frac{2\pi}{\lambda}d_{m,n}}, \tag{1}$$

where $m = 0,1,\ldots,M-1$, $n = 1,2,\ldots,N$, λ is the carrier wavelength and $d_{m,n}$ is the distance between the mth receiving antenna and the nth transmitting antenna. From the positional relationship between Tx and Rx, $d_{m,n}$ is given by

$$d_{m,n} = \sqrt{L^2 + d'^2_{m,n}} \approx L + \frac{d'^2_{m,n}}{2L}, \tag{2}$$

where $d'_{m,n}$ is the distance between the mth receiving antenna and the nth transmitting antenna when the receiving array is panned on the same plane as the transmitting array. $d'_{m,n}$ is expressed as (see Appendix A for details)

$$d'_{m,n} = \sqrt{\left(\frac{d_r}{2}\right)^2 + \left(\frac{d_t}{2}\right)^2 + \frac{d_r d_t}{2}\cos\left(\frac{2\pi n}{N} - \frac{2\pi m}{M}\right)}, \tag{3}$$

The elements $h_{m,n}$ of $\boldsymbol{H}$ are assembled as $\boldsymbol{h}_n = [h_{1,n},\ldots,h_{M,n}]^{\mathrm{T}}$ and $\boldsymbol{H} = [\boldsymbol{h}_1,\ldots,\boldsymbol{h}_N]$. The channel capacity of the LOS MIMO systems is then expressed as

$$C = \log_2\left(\left|\boldsymbol{I}_N + \frac{\rho}{\sigma^2 N}\boldsymbol{H}^{\mathrm{H}}\boldsymbol{H}\right|\right), \tag{4}$$

where ρ is the transmit power, σ^2 is the noise power, and M is greater than or equal to N.

According to matrix theory, the channel capacity reaches its upper bound when $\boldsymbol{H}^{\mathrm{H}}\boldsymbol{H}$ equals $M\boldsymbol{I}$. However, we found that the upper bound of the channel capacity cannot be reached when the number of antennas exceeds four, so instead we try to ensure $\boldsymbol{h}_i^{\mathrm{H}}\boldsymbol{h}_j \to 0$ by applying the minimum mean square error (MMSE) criterion. We further assume an equal number of RF chains at Rx and Tx; that is, $M = N = N_{\mathrm{RF}}$. When N_{RF} is given, $\eta^{\mathrm{opt}}_{N_{\mathrm{RF}}}$ can be expressed as follows:

$$\begin{aligned}\eta^{\mathrm{opt}}_{N_{\mathrm{RF}}} &= \arg\min_{\eta} \sum_{n_1=1}^{N_{\mathrm{RF}}} \sum_{\substack{n_2=1\\ n_2\neq n_1}}^{N_{\mathrm{RF}}} \left(\boldsymbol{h}^{\mathrm{H}}_{n_1}\boldsymbol{h}_{n_2}\right)^2 \\ &= \arg\min_{\eta} \sum_{n=2}^{N_{\mathrm{RF}}}\left(\sum_{m=1}^{N_{\mathrm{RF}}}\cos\left(\pi\eta\sin\frac{(n-1)\pi}{N_{\mathrm{RF}}}\sin\frac{(2m-n-1)\pi}{N_{\mathrm{RF}}}\right)\right)^2,\end{aligned} \tag{5}$$

where

$$\eta = \frac{d_r d_t}{\lambda L}. \tag{6}$$

As the UCA is symmetric, we need to analyze only the correlation between the first antenna and all other antennas. We define the average correlation coefficient as

$$\gamma = \frac{1}{N_{\mathrm{RF}}}\sqrt{\frac{\sum_{n=2}^{N_{\mathrm{RF}}}\left(\sum_{m=1}^{N_{\mathrm{RF}}}\cos\left(\pi\eta\sin\frac{(n-1)\pi}{N_{\mathrm{RF}}}\sin\frac{(2m-n-1)\pi}{N_{\mathrm{RF}}}\right)\right)^2}{N_{\mathrm{RF}}-1}}. \tag{7}$$

* Corresponding author (email: fanjc0114@gmail.com, luoxm@mail.xjtu.edu.cn)

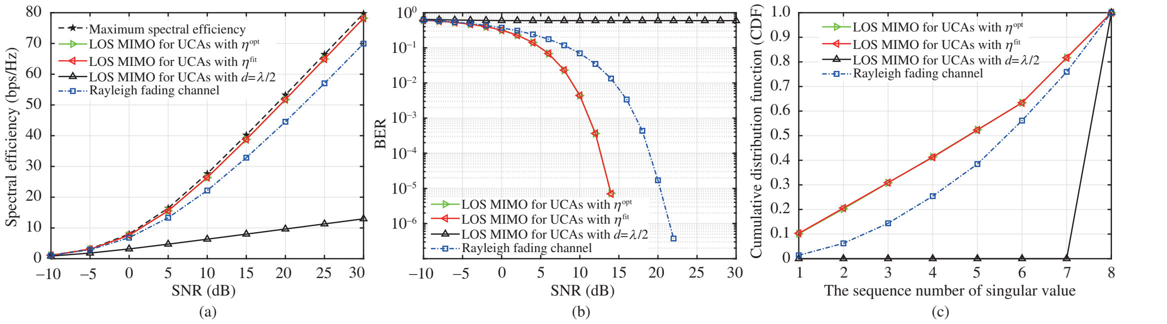

Figure 1 (Color online) Simulation results. (a) SE comparison when $N_{\rm RF}=8$; (b) BER comparison when $N_{\rm RF}=8$; (c) CDF curve of singular value.

In (7), the average correlation coefficient is determined by summing some trigonometric functions. First, we explore a simple sum of trigonometric functions as

$$y_{\rm sum}=\sum_{\omega=1}^{K}\cos(\omega x). \tag{8}$$

A simple numerical simulation confirmed that $y_{\rm sum}$ first decreased and then fluctuated with increasing x. The first minimum is equal to the global minimum. Note that Eqs. (7) and (8) present similar characteristics. Therefore, as η increases, Eq. (7) should also decrease first and then fluctuate. We verify this hypothesis in Appendix B. We choose the first minimum point as the approximate optimal solution of η, and denote it by $\eta^{\rm opt}$. We find $\eta^{\rm opt}$ by a grid search and count the number of $\eta^{\rm opt}$ solutions corresponding to $N_{\rm RF}$. The results are shown in Appendix C.

A simplified algorithm. Although the grid search provides the approximate optimal solution $\eta^{\rm opt}$, its complexity is problematic. Therefore, we developed a simple algorithm for obtaining $\eta^{\rm opt}$. In Appendix D, we prove that $\eta^{\rm opt}$ and $N_{\rm RF}$ are roughly linear with respect to each other. We thus obtain the relationship between $\eta^{\rm opt}$ and $N_{\rm RF}$ by a linear fitting method. The linear fitting results of the data $\eta^{\rm opt}$ are shown in Appendix C. The fitting equation is

$$\eta^{\rm fit}=0.2988\times N_{\rm RF}-0.391. \tag{9}$$

Note that $\eta^{\rm fit}$ is obtained by simple multiplication and addition operations. We can assume that the Tx and Rx arrays have the same diameter d_r. Substituting (6) into (9), we get $d_t=d_r=\sqrt{(0.2988\times N_{\rm RF}-0.391)\,\lambda L}$.

In this case, the area of the UCA at Tx is

$$S_t=\pi\left(\frac{d_t}{2}\right)^2=\frac{(0.2988\times N_{\rm RF}-0.391)\,\pi\lambda L}{4}. \tag{10}$$

When the carrier frequency λ and the distance L between Tx and Rx are given, Eq. (10) describes a linear relationship between the size of the proposed UCA and the number of RF chains.

Simulation results. To evaluate the performance of the proposed UCA, we adopted the spectral efficiency (SE), bit error rate (BER), and cumulative distribution function (CDF) of singular values. The carrier frequency f was 75 GHz. The distance L between Tx and Rx was 100 m. Eight RF chains and eight antennas were set at both Tx and Rx.

We compared three UCA structures: (1) the proposed UCAs designed with $\eta^{\rm opt}$, and $d_t^{\rm opt}=d_r^{\rm opt}=\sqrt{\eta^{\rm opt}\lambda L}=0.8876$ m, (2) the proposed UCAs designed with $\eta^{\rm fit}$, and $d_t^{\rm fit}=d_r^{\rm fit}=\sqrt{\eta^{\rm fit}\lambda L}=0.8943$ m, and (3) the UCAs designed with a half-wavelength antenna spacing. In addition, we generated a special channel for the performance evaluation, namely, an 8×8 Rayleigh fading channel. The simulation details are presented in Appendix E.

As shown in Figure 1, the UCA designed with $\eta^{\rm opt}$ and $\eta^{\rm fit}$ achieved similar performances, and both outperformed the Rayleigh fading channel. Therefore, $\eta^{\rm fit}$ is a suitable proxy of $\eta^{\rm opt}$.

Conclusion. We explored the possibility of achieving a full-rank channel matrix for UCAs with more than four antennas. First, the correlation between the antennas was minimized under the MMSE criterion. We then approximated the optimal diameter based on the properties of correlation coefficients. The size of the proposed UCA is a linear function of the number of RF chains. Finally, we incorporated this linear feature in a simplified algorithm.

Acknowledgements This work was partially supported by National Natural Science Foundation of China (Grant No. 61671367), Key Research and Development Plan of Shaanxi Province (Grant No. 2018GY-003), and Research Foundation of Science and Technology on Communication Networks Laboratory.

Supporting information Appendixes A–E. The supporting information is available online at info.scichina.com and link.springer.com. The supporting materials are published as submitted, without typesetting or editing. The responsibility for scientific accuracy and content remains entirely with the authors.

References

1 Zhang P Z, Yi C, Yang B S, et al. In-building coverage of millimeter-wave wireless networks from channel measurement and modeling perspectives. Sci China Inf Sci, 2020, 63: 180301
2 Kang M, Alouini M S. Capacity of MIMO Rician channels. IEEE Trans Wirel Commun, 2006, 5: 112–122
3 Xue C L, He S W, Ou F F, et al. Asymmetric subarray structure design for mmWave LoS MIMO communication systems. In: Proceedings of IEEE/CIC International Conference on Communications in China (ICCC), 2016
4 Zhou L, Ohashi Y. Low complexity linear receivers for mmWave LOS-MIMO systems with uniform circular arrays. In: Proceedings of the 80th Vehicular Technology Conference (VTC2014-Fall), 2014
5 Zhu L, Zhu J. Optimal design of uniform circular antenna array in mmWave LOS MIMO channel. IEEE Access, 2018, 6: 61022–61029